Design and Characterization of a Littrow Configuration External Cavity Diode Laser

Wenxian Hong

under the direction of
Professor Oskar J. Painter
California Institute of Technology

Abstract

An enhanced tunable Littrow-configuration external-cavity diode laser (ECDL) is constructed from inexpensive commercial components and then characterized. The introduction of an additional mirror parallel to the diffraction grating allows the laser to be tuned without changing the direction of the output beam. The 785 nm ECDL has a typical power output of 4 mW at 56.0 mA of current input with an effective tuning range of 13 nm and exhibits excellent output-beam directional stability. An upper limit on its linewidth is placed at 63.0 MHz.

1 Introduction

External-cavity diode lasers (ECDL) have widespread applications in optical and atomic physics. Such lasers make use of inexpensive yet efficient semiconductor diode lasers which are pumped by electrical energy [4]. The diode is coupled to an external cavity that incorporates a diffraction grating as a wavelength-selective element, which then provides frequency-selective optical feedback to the diode laser via its antireflection-coated output facet. This concept of frequency selective feedback allows the laser to achieve narrow linewidth and remarkable tunability. Typically, such feedback is obtained through diffraction gratings in either the Littrow or Littman-Metcalf configurations.

In the more popular Littrow configuration, shown in Figure 1, the grating is aligned such that the first-order diffraction from the grating is coupled directly back into the laser while the zeroth-order diffraction is reflected as the output beam. The lasing wavelength is dependent on the angle of the incident laser beam with respect to the grating, otherwise known as the Littrow angle θ. Thus, by changing the Littrow angle, precise wavelength tuning can be achieved. The Littrow configuration offers the advantage of high efficiency and power but also faces problems of mode-hopping and beam angular displacement as the grating angle is adjusted.

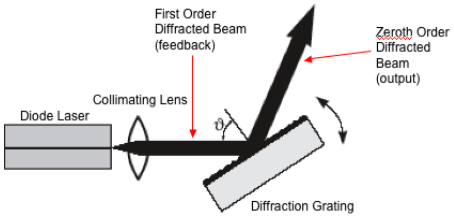

Figure 1: Schematic diagram of external cavity in Littrow configuration. Adapted from [10]

On the other hand, the Littman-Metcalf configuration [8, 9], as depicted in Figure 2, utilizes a diffraction grating at grazing incidence. The first-order diffraction beam goes to an additional mirror, which then reflects the beam back to the grating and into the diode laser as optical feedback. Tuning is achieved by varying the mirror angle instead of the grating angle, allowing the grating, and thus the zeroth-order output beam, to remain fixed as wavelength is changed. Relative to the Littrow design, the Littman-Metcalf configuration overcomes the problems of mode-hopping and beam angular displacement but does not share as high an output efficiency. Furthermore, the additional components involved and its design complexity prevent it from surpassing the widespread prevalence of the relatively simpler yet adequately effective Littrow arrangement.

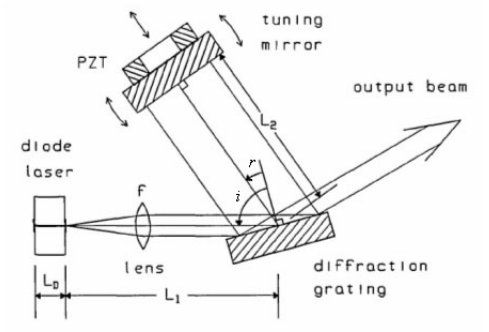

Figure 2: Schematic diagram of an external-cavity diode laser in the Littman-Metcalf configuration [7]

Here, an external-cavity diode laser is constructed based on the Littrow configuration, in close reference to the design of Hawthorn, Weber, and Scholten [6]. Minor modifications have been made to circumvent the problem of beam angular displacement and to produce a fixed-direction output beam. With a fixed output beam, the flexibility of the ECDL is enhanced as the output beam is now able to undergo fiber coupling for delivery to distant applications. The power output and linewidth of the modified ECDL are then determined using instruments such as an optical spectrum analyzer (OSA), a scanning Fabry-Perot interferometer (SFP), and a Michelson interferometer. This modified design is not only low-cost and simple to build, but also produces single-mode emissions of varying wavelengths sufficient for most applications, particularly pertaining to high-resolution, broadband spectroscopy.

2 Design and Construction

The design of the external-cavity diode laser presented here takes advantage of a simple modification of standard Littrow-configured ECDLs to produce a fixed-direction output beam without significant output-power loss. The ECDL, which was named Promise (Figure 3), consists of a 70 mW, 785 nm laser diode (Sanyo DL7140-201S) and aspheric collimating lens (Thorlabs C230TM-B, $f = 4.5$ mm and 0.55 NA) mounted in a collimation tube (Thorlabs LT230P-B). The threaded collimation tube allows for accurate focusing of the collimating lens and also aligns the lens axis with the laser diode axis. The diode-tube assembly is then fixed to the back plate of a modified optical mount (Newport U100-P2K). The modifications on the optical mount include the tapping of three holes into the front plate and the removal of a square section of the plate. The diffraction grating used (Thorlabs GR13-1208) is gold-coated and blazed at 28° with 1200 lines/mm on a 12.7 mm × 12.7 mm × 6 mm substrate. A grating mount is constructed to hold the diffraction grating and is subsequently attached to the front plate of the modified U100-P2K. The grating is vertically and horizontally adjusted by the mirror mount actuators for coarse wavelength tuning.

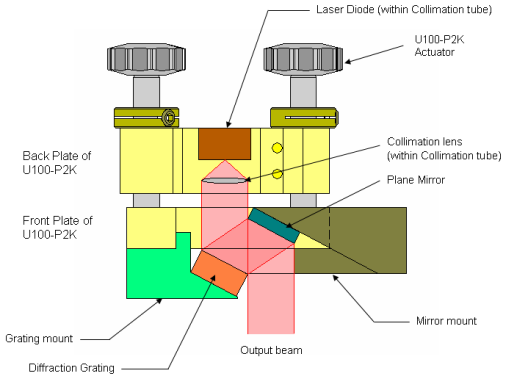

Figure 3: Schematic diagram of the enhanced Littrow-configuration external-cavity diode laser (Promise), as viewed from above

The main modification made to ensure a fixed-direction output beam is the addition of a single plane mirror (Newport 05SD520ER.2) parallel to the tuning diffraction grating and located rigidly with respect to it. This is done by attaching the mirror to a mirror mount that is then secured to the front plate of the U100-P2K. The laser beam reflects from the grating and then from the mirror, thus replacing an otherwise large angular beam displacement with a negligible translational beam displacement. When the grating is rotated by $\Delta\theta$, the beam reflected by the grating is rotated by twice that angle, or $2\Delta\theta$, by the law of specular reflection. Since the mirror rotates by the same angle as the grating, when the reflected beam from the grating strikes the mirror, it is again reflected back by $2\Delta\theta$, such that the output beam remains relatively fixed. This concept of adding a mirror to prevent beam displacement has also been employed in the design of Hawthorn, Weber and Scholten [6] and is an improvement on the

previous design by Arnold, Wilson, and Boshier [2]. However, due to the differences in blaze angle of gratings used, minor design changes were made to the positions of the mirror and grating so that they were parallel and did not obstruct the output beam.

The compact nature of the Promise ECDL also provides for simple and efficient temperature regulation of the entire system using a Peltier thermoelectric cooler (Melcor CP1.4-71-045L). A 10 kΩ thermistor (Thorlabs TH10K) attached to the collimation tube assembly provides feedback to the thermoelectric cooler via a temperature controller, thus ensuring reasonable thermal stability. Thermal paste is applied at each interface to ensure optimal thermal conductivity and efficient cooling of the setup. In addition to the thermistor used for temperature control, another temperature sensor (LM35) on the collimation tube gives independent readouts. Other improvements made to the ECDL system include the use of a massive aluminum metal base/heat sink to provide inertial and thermal damping. The ECDL setup is isolated from the optical table by placing a layer of Sorbothane beneath the baseplate as well as by enclosing the laser with an aluminum cover, which is also isolated from the laser by Sorbothane. This dampens acoustic noise and shields the laser from air currents, thus providing for great stability and precision of the instruments.

The design of Promise described above calls for the modifications of several components and the construction of other new parts. During the time spent waiting for the machining of components, a second ECDL, named Prowl, was constructed using existing components. The concept of the latter laser remains the same as the former, making use of the modified Littrow configuration, which introduces the plane mirror that moves simultaneously with the rotation of the diffraction grating. The only visible difference is that instead of containing the entire ECDL system within a single U100-P2K mount, the Prowl design makes use of the back plate of one U100-P2K mount to hold the laser diode and another unmodified U100-P2K mount to provide for manual translation of the grating and mirror. All essential aspects of the laser, such as the thermoelectric cooler, have been included, though less important components such as the independent temperature sensor have been omitted. These minor modifications will only serve to lengthen the cavity length slightly, reducing the mode spacing of the external cavity, but should not significantly hinder the performance of the laser. Thus, the ECDL design of Prowl is likely to demonstrate the strengths of the modified Littrow configuration to as great an extent as the initially intended design of Promise.

3 Methodology

Upon construction, the lasers were characterized based on certain performance indicators, namely output power, tuning range, output-beam directional stability, and linewidth. A battery of tests was run using various devices to analyze the laser performance, the methodologies of which will be presented in this section. However, due to time constraints, the experiments outlined mainly pertain to the performance characteristics of Prowl. Nevertheless, similar experiments can be conducted with the Promise design to evaluate its effectiveness when time permits.

3.1 Alignment of Feedback

The key to the Littrow configuration is the back-coupling of the first-order diffraction beam from the grating into the laser diode. Without this feedback, the Littrow laser cannot achieve single-mode emission and will lase at a wavelength set by the gain peak of the semiconductor active region. Thus, it is critical to first align the feedback beam before carrying out further experiments. Preliminary alignment is done visually by rotating the actuators and merging the secondary feedback and output beams into a single bright spot on a screen at the output of the laser. Good alignment is confirmed by inspecting the laser spectrum using an optical spectrum analyzer or scanning Fabry-Perot interferometer, and modifications are made until single-mode emission is obtained. Aligning the feedback beam is also considerably easier when the laser is close to its lasing threshold, since the laser is most sensitive to feedback at this point. When the feedback beam is well aligned, interference fringes are expected in the output beam and the laser remains single-mode with temperature and current changes.

3.2 Optical Spectrum Analyzer

An optical spectrum analyzer is an instrument that displays the wavelength-dependent intensity of input light. This is achieved by means of a rotating diffraction grating that deflects light of different

wavelengths at different angles. A fixed detector measures the intensity of incident light at a given angle, thus determining the wavelength-dependent intensity as the diffraction grating is rotated. Using this instrument, we are able to determine the effective tuning range of the Prowl ECDL as well as its output power.

The output beam of the Prowl ECDL was directed to a fiber coupler leading to the OSA located 70 cm from the output mirror of the laser. The ECDL actuators were rotated so that the diffraction grating was tilted about an axis parallel to its grooves, thereby giving rise to coarse wavelength tuning. The laser wavelength was continuously tuned until a significant mode-hop back to the central gain peak was detected, signaling that the wavelength-dependent gain had overcome the wavelength-selective influence of the feedback. This demarcated the upper and lower limits of the ECDL tuning range. Five digital screen shots were taken across the entire tuning range, spaced at approximately equal wavelength intervals. The linewidth of the laser can also be approximated from a single normalized digital scan. Throughout all these experiments, the temperature was regulated by the thermoelectric cooler at a thermistor resistance of 11.0 kΩ, corresponding to a relatively constant temperature of 23.9°C, so as to minimize the adverse effects of thermal drift.

3.3 Scanning Fabry-Perot Interferometer

The scanning Fabry-Perot interferometer provides a greater resolution for the linewidth measurement as compared to the OSA. The SFP comprises a regular Fabry-Perot etalon with a fixed mirror arm and a piezoelectric actuator attached on the other partially transmitting mirror arm. As voltage is applied across the piezostack, the Fabry-Perot cavity length constantly changes by a small displacement and thus varies the standing wavelengths within the cavity. A detector measures the intensity of light that eventually leaves the cavity via the partially transmitting mirror, while an oscilloscope displays the intensity of light against the voltage applied to the piezostack, which can later be related to frequency.

The SFP used in the characterization of Prowl is the Tropel Model 240 Spectrum Analyzer, with a finesse of 200 at 700 nm and a free spectral range (FSR) of 1.5 GHz. The output beam from the Prowl ECDL is directed through the SFP to obtain a repeating series of Lorentzian lineshape functions. After the normalization of waveforms, the linewidth of a single wave is then determined. The SFP is also particularly useful in ascertaining the quality alignment of the grating feedback, as multi-mode emission lines can be clearly resolved.

3.4 Michelson Interferometer

In a Michelson interferometer, a beam splitter divides the incident waves from a light source into two samples, which are then directed along separate paths. Each beam of light travels a different path length along each arm of the interferometer, acquiring a relative phase difference in the process. When the beams are reflected back to the beam splitter, they recombine and interfere to produce a interference pattern. By examining the interference in the recombined beam, information on the source spectrum can be obtained. Here the Michelson interferometer is employed to observe the visibility of fringes produced at the output beam. As the relative path length is lengthened by moving one of the arms away from the beam splitter, the beam in the arm gradually loses coherence, causing the fringes to oscillate between constructive and destructive interference and leading to an overall decrease in fringe visibility. A photodetector placed at the recombined beam measures the intensity of the fringes and translates the data to an oscillating voltage output. The envelope of the oscillating output is then displayed on an oscilloscope.

This decay in fringe visibility occurs as a result of broadening effects, in particular Lorentz broadening. Lorentz broadening (or lifetime broadening) results from species in excited states having finite lifetimes. From Heisenberg's uncertainty principle, the product of uncertainties in energy levels and lifetimes is on the order of $\hbar$. Hence, the finite lifetime of an excited species leads to a spectrum of energy emitted when the species returns to ground state, giving rise to broadening of the laser waveform. The fringe visibility function, $V(\tau)$, for a Lorentz broadened wave is described by the exponential curve

$$V(\tau) = \exp -\pi\tau\Delta\nu/2, \tag{1}$$

where τ is the time difference between the two paths and $\Delta\nu$ is the linewidth of the laser mode [3].

The Michelson-interferometer measurements were carried out with a current input of 40.1 mA and a thermistor resistance of 11.0 kΩ. One arm of the interferometer was lengthened by 45 cm using a Unislide carriage, and the fringe visibility curve was

plotted by the oscilloscope. Three repetitions were carried out with the same interferometer alignment configuration and with the Unislide moving at the same velocity. By fitting the empirical data obtained from the oscilloscope on a similar exponential, the linewidth of the laser can then be calculated.

4 Performance

4.1 Tuning range of ECDL

The digital screenshots taken from the OSA were compiled using MATLAB to describe the tuning range of the Prowl ECDL. At 56.0 mA, the wavelength of laser output can be tuned over a 11 nm range from 775 nm to 786 nm by rotating the grating alone. At lower current inputs of 37.8 mA, wavelength tunability can be further extended to a wider range of 13 nm between 774 nm and 787 nm, as shown in Figure 4. A qualitative explanation of this phenomenon stems from the knowledge that the wavelength at which spontaneous emission occurs is dependent on the gain spectrum, while the lasing wavelength is dependent on both the gain spectrum and reflectivity of the grating. Thus, at higher currents, the broad gain spectrum tends to overwhelm the influence of the narrow band grating reflectivity, making it more difficult for the ECDL to lase based on frequency-selective feedback. However, when the current input nears the lasing threshold limit at 33.0 mA (Figure 5), the tuning range of the ECDL once again shrinks slightly to 12 nm (774–786 nm). This is because the amplitude of the gain spectrum decreases with lower currents. Thus, the range of wavelengths at which gain exceeds loss (i.e., possible lasing wavelengths) is reduced, limiting the tuning range of the ECDL.

It is also worthwhile to note that the gain spectrum of the ECDL, although approximated by a Gaussian in Figures 4 and 5, is actually slightly asymmetrical. This is because the semiconductor material in the laser diode absorbs at shorter wavelengths compared to the wavelengths at which it emits. Since gain is proportional to the difference between emission and absorption of photons, higher gain is obtained at longer wavelengths, resulting in a steeper gradient on the gain spectrum at shorter wavelengths and an asymmetrical gain spectrum shape.

These wavelength measurements do not take into account the effect of temperature variations, which should allow the laser to tune over an even wider

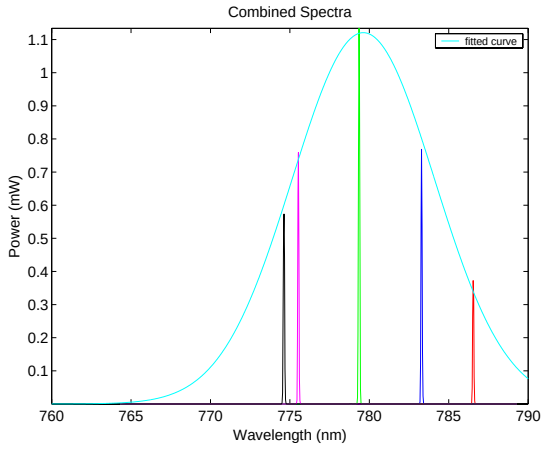

Figure 4: OSA plot of intensity against wavelength at 37.8 mA, showing the tuning range of the ECDL. The fitted curve represents the projected gain spectrum of the laser.

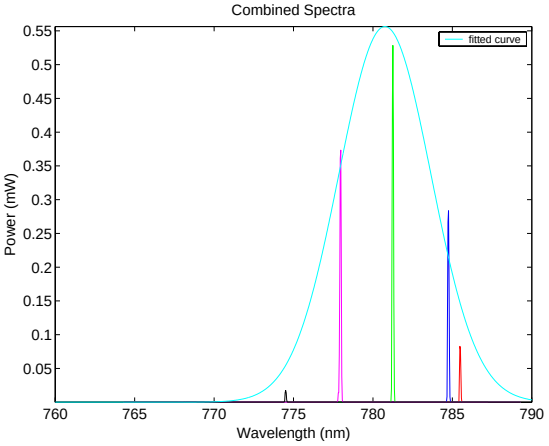

Figure 5: OSA plot of intensity against wavelength at 33.0 mA, showing the tuning range of the ECDL. The fitted curve represents the projected gain spectrum of the laser.

range. Nevertheless, the wavelength-tunability values obtained for the Prowl ECDL are reasonably comparable to commercial standards, demonstrating the feasibility of the design.

4.2 Output power of ECDL

With the laser wavelength tuned to the gain peak, the output power of the Prowl ECDL was measured to be

approximately 1.1 mW at 37.8 mA of current input and about 4.0 mW with 56.0 mA of current. It may seem surprising that the power output of the Prowl ECDL is a mere fraction of the typical power output of the 70 mW laser diode. However, this is expected since the diffraction grating used has a high efficiency of 60%–80% at blaze wavelength. Consequently, most of the diode power output will be reflected back into the diode by the grating instead of being directed into the zeroth-order beam, resulting in the observed low power output. However, the small power coupled out of the ECDL is sufficient to accurately characterize the laser and should not pose too great a concern.

4.3 Output-beam directional stability of ECDL

The output-beam directional stability of the Prowl ECDL was demonstrated by monitoring the tuning of wavelength as the grating is rotated using an OSA located 70 cm from the laser. Despite the high sensitivity of the OSA fiber coupler to beam misalignment, the full tuning range of 13 nm was scanned successfully by adjusting the grating angle, without any need for realignment. This wavelength variation will normally displace the output direction of the laser beam by about 0.45° and cause a lateral translation of 5.5 mm at the fiber coupler. However, with the additional mirror, the lateral displacement of the output beam for a small change $\Delta\theta$ in grating angle is now given by $\Delta x \sim 2L\Delta\theta$, where L is the distance the beam travels between the grating and mirror.

Given that L (~ 3 cm) is far smaller than 70 cm, the geometric ingenuity of the Prowl design has not only enabled the angle of output beam to remain unchanged, but also made the lateral displacement negligible at approximately 0.47 mm. Such minute shifts are insignificant for most applications, indicating the success of the Prowl design in maintaining a fixed-direction output beam.

4.4 Linewidth of ECDL

An attempt to measure the linewidth of the Prowl ECDL was first made using the OSA. A single Lorentzian lineshape waveform obtained at the laser emission wavelength at 60.0 mA was plotted and normalized. By examining the full width half maximum (FWHM) of the waveform, the linewidth of Prowl was measured to be approximately 0.08 nm, or 39 GHz, at 60.0 mA (Figure 6), which corresponds to the resolution bandwidth of the OSA. Intuitively, this value is likely to be too large as commercial lasers of the same standard generally have linewidths in the order of kHz or MHz. Hence, it is reasonable to infer that the OSA lacks the necessary resolution bandwidth to resolve the narrow linewidth of the laser.

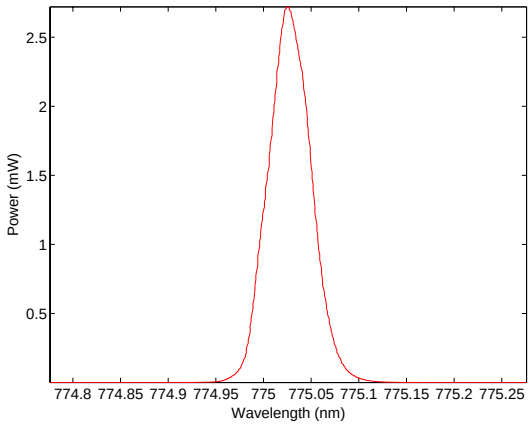

Figure 6: Measurement of linewidth using the optical spectrum analyzer. Note that the linewidth is limited by the resolution bandwidth of the OSA (~ 0.08 nm).

Therefore, the SFP was employed to determine the linewidth of Prowl to greater precision. After single-mode emission was obtained, two adjacent peaks were normalized and spaced at nine divisions apart by adjusting the x-axis scale of the oscilloscope (Figure 7a). Since the FSR of the SFP is given as 1.5 GHz, the voltage separation on the x-axis between the peaks can now be related to frequency. The FWHM is then measured on the normalized scale. Figure 7b shows that at 50 mA, the FWHM of the waveform is measured to be approximately 0.7 of a division. Using simple proportion calculations, the FWHM corresponds to about 120 MHz. At 70 mA, the FWHM is exactly 1 division long, or 170 MHz in terms of frequency.

Now, it is imperative to note that the FWHM measurements obtained could refer to either the Prowl ECDL linewidth or scanning Fabry-Perot linewidth. In order to distinguish between the two, the effect of tilting the SFP on the waveform obtained is examined. By tilting the SFP slightly, the reflectivity of the mirrors drops sharply, resulting in a significantly lower finesse. Recalling the relationship $\Delta\nu = \nu_{\mathrm{FSR}}/F$, a lower finesse will give rise to a greater Fabry-Perot linewidth. So, if the Fabry-Perot linewidth were much narrower than the

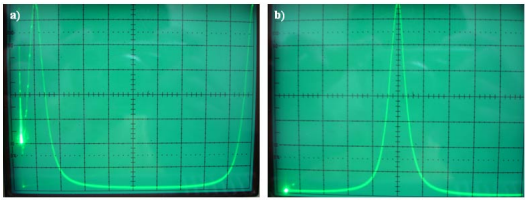

Figure 7: a) Normalization of adjacent peaks on SFP oscilloscope. b) Measurement of linewidth on normalized scale using the SFP.

laser linewidth, any slight increase in the Fabry-Perot linewidth should still not alter FWHM measurements significantly. However, it is indeed observed that by changing the angle of incident light on the SFP, the FWHM measurements do not remain constant. Therefore, one can infer that the Fabry-Perot linewidth must be bigger than that of the laser. As such, even though the SFP measurements have narrowed down the laser linewidth by a factor of 300, this is still insufficient to totally resolve the narrow laser linewidth.

This result is not surprising, as the Tropel Model 240 Spectrum Analyzer is designed for wavelengths ranging from 600 nm to 700 nm, which is not within the wavelength range of the ECDL (~ 780 nm). The dielectric mirrors of the SFP have a narrow bandwidth of wavelengths for which they have high reflectivity, and beyond this bandwidth, the finesse of the SFP drops drastically (a value of 100 MHz for the Fabry-Perot linewidth would actually imply that the finesse has fallen from 200 to 15). In order to provide greater resolution for the laser linewidth, a SFP with a higher finesse at the required wavelength should be used. However, the measurements of the SFP have served a useful purpose in placing an upper boundary on the linewidth of the laser, meaning that the linewidth cannot exceed frequencies on the order of 100 MHz.

The linewidth measurements obtained from the Michelson interferometer experiment were slightly more satisfactory. Assuming that the decay curve obtained from the oscilloscope follows the exponential in Equation (1), we are able to describe the exponential curve using the initial voltage V_0 and the final voltage V_f. Equation (1) then changes to

$$V_0 \exp -\pi\tau\Delta\nu/2 = V_f. \tag{2}$$

Solving for $\Delta\nu$ yields

$$\Delta\nu = -\frac{2}{\pi\tau} \ln \frac{V_f}{V_0}. \tag{3}$$

Substituting the relevant values of τ, V_0 and V_f into Equation (3), allows the linewidth of the laser to be easily calculated. Table 1 shows the results of the Michelson-interferometer experiments conducted and the linewidth values obtained.

τ / ns	V_0 / V	V_f / V	$\Delta\nu$ / MHz
3.0	11.6	8.1	76.2
3.0	11.1	7.6	80.4
3.0	10.9	7.7	73.8

Table 1: Summary of Michelson interferometer experiment.

By averaging the three linewidth values obtained, the average linewidth of the laser is calculated to be 76.8 MHz. This is a conservative estimate, but nevertheless further narrows the linewidth range of the laser. However, undulations observed in the empirical decay curve have rendered the linewidth values less accurate than desired. This problem can be overcome by only considering part of the decay graph, where the progression seems relatively exponential. Given that the average velocity of the Unislide carriage was $0.20\ \mathrm{cm \cdot s^{-1}}$, and that the timeframe considered was 70 s, a new value of τ was calculated. Table 2 shows the results of the linewidth calculations under these new conditions.

τ / ns	V_0 / V	V_f / V	$\Delta\nu$ / MHz
0.93	8.8	8.1	56.7
0.93	8.4	7.6	68.5
0.93	8.4	7.7	63.9

Table 2: Linewidth calculations after additional considerations on the exponential nature of the data curve. Note that the distance travelled by the Unislide carriage is no longer 45 cm.

This time, by averaging the three linewidth values, a narrower average linewidth of 63.0 MHz is obtained. Considering the mechanical noise produced by the Unislide carriage while in motion, which may disturb the laser, as well as the limited ability of such Michelson interferometer experiments to measure linewidth, a linewidth value below 100 MHz

demonstrates the success of this particular experiment. In conclusion, after using the three different instruments, OSA, SFP, and Michelson interferometer, the Michelson interferometer proved to be most precise, and the final upper bound on the linewidth was set at 63.0MHz.

5 Discussion

Prowl has clearly proven itself to be feasible for general use as a tunable laser, from its wide tuning range, mechanical stability and narrow linewidth. One of the biggest advantages of the design is that it primarily makes use of inexpensive, readily available optical components. The total cost of construction was under US$1000, comparatively cheaper than most commercial Littrow-configured ECDLs. Moreover, the ready accessibility of the different parts makes the laser especially simple to construct. The additional mirror introduced has also worked superbly to allow for coarse tuning without alteration of alignment, greatly enhancing the versatility of the conventional Littrow ECDL. Both the Promise and Prowl lasers will be used subsequently in experiments pertaining to atomic spectroscopy and laser cooling and have helped pave the way for other novel designs of compact ECDLs.

A significant problem faced in the construction of the Prowl laser, however, was the ease with which the laser diode could be blown. This occurred despite the use of a current controller that protects the laser diode with a shunting circuit by dissipating current transients when the power cable is detached. The blowing of the diode can be attributed to the loose fit between the diode ends and diode socket. When the diode socket was accidentally disconnected, there was no protective circuitry to prevent strong current transients from entering the diode and ruining its intrinsic material properties. Thus, future design considerations should incorporate a firm coupling to give a tighter fit between the diode and the socket.

Several other improvements can be made to the existing Prowl or Promise design to further extend its applications. These include the installation of a piezostack on the front plate of the U100-P2K and a piezodisk on the diffraction grating, so as to enable fine continuous wavelength tuning across the cavity mode spacing. Secondly, to increase the existing power output, a diffraction grating with lower efficiency at blaze wavelength could be used so that more power is coupled into the output beam instead of the feedback beam. Alternatively, the grating could be deliberately misplaced away from its blaze angle. Lastly, smoother tuning and wider wavelength variations can be achieved by applying an antireflection (AR) coating to reduce the reflectivity of the laser diode output facet. External-cavity lasers using optimally AR coated diodes have achieved continuous tuning ranges of several THz [1]. Thus, an appropriate AR coating will appreciably enhance the tunability of the ECDL.

Future studies could begin with the characterization of the Promise design, since time constraints have prevented the construction and testing of this laser. A comparison could be made between the designs of Promise and Prowl to evaluate the strengths and weaknesses of both lasers. Furthermore, three methods of linewidth measurement have been presented, although these are not as accurate as desired. Higher linewidth resolution could be provided by heterodyning and photomixing methods, where the beat frequency of two ECDLs operating at nearly the same frequency is measured. As an extension, both lasers can be locked and stabilized by the Zeeman effect and the radiofrequency (rf) beat between them observed with an avalanche photodiode [12].

6 Conclusion

The design of a compact tunable Littrow-configured external-cavity diode laser was described. Empirical data from performance tests indicated that the Prowl ECDL has an effective tuning range of 13 nm, a typical output power of 4 mW and a linewidth of at most 63.0 MHz. The laser also exhibited exceptional output-beam directional stability due to the introduction of a plane mirror parallel to the grating. These superior characteristics of Prowl testify to the advantages of the enhanced ECDL design. The simple modifications presented here can be applied to existing Littrow-configuration ECDLs, and the design holds exciting prospects for future applications in atomic and optical physics.

7 Acknowledgments

I would like to extend my sincerest thanks to my mentor, Professor Oskar J. Painter of the California Institute of Technology, and his graduate students Orion Crisafulli and Raviv Perahia for the invaluable guidance and assistance they provided in the course of the

project. Also, I would like to thank my tutor, Dr. John Rickert, and the staff of the Research Science Institute at Caltech for their input and suggestions as well as help rendered in times of need. Finally, I would like to express my heartfelt gratitude to the Center for Excellence in Education and the Ministry of Education, Singapore, for giving me this unique opportunity to enrich myself and expand my horizons.

References

[1] A. Andalkar, S.K. Lamoreaux and R.B. Warrington. Improved external cavity design for cesium D1 (894 nm) diode laser. Review of Scientific Instruments 71 (2000), no. 11, 4029–4031.

[2] A.S. Arnold, J.S. Wilson and M.G. Boshier. A simple extended-cavity diode laser. Review of Scientific Instruments 69 (1998), no. 3, 1236–1239.

[3] M. Born and E. Wolf. *Principles of Optics.* 7th ed. Cambridge University Press, Cambridge, United Kingdom (2002).

[4] L.A. Coldren and S.W. Corzine. *Diode Lasers and Photonic Integrated Circuits.* John Wiley & Sons, Inc., New York, NY (1995).

[5] T.M. Hard. Laser wavelength selection and output coupling by a grating. Applied Optics 9 (1970), no. 8, 1825–1830.

[6] C.J. Hawthorn, K.P. Weber and R.E. Scholten. Littrow configuration tunable external cavity diode laser with fixed direction output beam. Review of Scientific Instruments 72 (2001), no. 12, 4477–4479.

[7] K.C. Harvey and C.J. Myatt. External-cavity diode laser using a grazing-incidence diffraction grating. Optics Letters 16 (1991), no. 12, 910–912.

[8] M.G. Littman and H.J. Metcalf. Spectrally narrow pulsed dye laser without beam expander. Applied Optics 17 (1978), no. 14, 2224–2227.

[9] K. Liu and M.G. Littman. Novel geometry for single-mode scanning of tunable lasers. Optics Letters 6 (1981), no. 3, 117–118.

[10] O.I. Permyakova, A.V. Yakovlev, and P.L. Chapovsky. Simple external cavity diode laser. To be published (2003).

[11] B.E.A. Saleh and M.C. Teich. *Fundamentals of Photonics.* John Wiley & Sons, Inc., Canada (1991).

[12] C.E. Wieman and L. Hollberg. Using diode lasers for atomic physics. Review of Scientific Instruments 62 (1991), no. 1, 1–20.